

Electronic Supplementary Material

Enhanced charge extraction for all-inorganic perovskite solar cells by graphene oxide quantum dots modified TiO₂ layer

Yili Liu¹, Guoliang Che¹, Weizhong Cui¹, Beili Pang (✉)¹, Qiong Sun¹, Liyan

Yu (✉)^{1,2}, Lifeng Dong (✉)^{1,2}

1 College of Materials Science and Engineering, Qingdao University of Science and Technology, Qingdao 266042, China

2 Department of Physics, Hamline University, St. Paul 55104, USA

E-mails: pangbl@qust.edu.cn (Pang B); liyanyu@qust.edu.cn (Yu L); donglifeng@qust.edu.cn (Dong L)

Table S1. Comparison of CsPbBr₃ PSCs with graphene materials and QDs.

Device structure	PCE/(%)	Ref.
FTO/c-TiO ₂ /m-TiO ₂ /CsPb _{1-x} Ag _x Br ₃ /carbon	6.92%	S1
FTO/c-TiO ₂ /m-TiO ₂ /CsPbBr ₃ : g-C ₃ N ₄ /carbon	8.00%	S2
FTO/TiO ₂ /CsPbBr ₃ /carbon	5.44%	S3
FTO/TiO ₂ /CsPbBr ₃ -CsPb ₂ Br ₅ /Spiro-OMeTAD/Ag	8.34%	S4
FTO/c-TiO ₂ /m-TiO ₂ /CsPbBr ₃ /MoS ₂ QDs/carbon	6.80%	S5
FTO/c-TiO ₂ /m-TiO ₂ /CsPbBr ₃ /BHJ/carbon	8.94%	S6
FTO/ZnO/CsPbBr ₃ -CsPb ₂ Br ₅ /PCBM/Ag	6.81%	S7
FTO/c-TiO ₂ /CsPbBr ₃ /spiro-MeOTAD/Au	8.65	S8
FTO/a-Nb ₂ O ₅ /CsPbBr ₃ /CuPC/carbon	5.74	S9
FTO/c-TiO ₂ /CsPbBr ₃ /carbon	7.81	S10
FTO/c-TiO ₂ /CsPbBr ₃ /buffer layer/P3HT/Au	7.90	S11
FTO/TiO ₂ /CsPb _{0.998} Co _{0.002} Br ₃ /Spiro-OMeTAD/Au	8.57	S12
FTO/Sr-TiO ₂ /CsPbBr ₃ /Carbon	7.22	S13
FTO/c-TiO ₂ /m-TiO ₂ /InBr ₃ :CsPbBr ₃ /carbon	6.48	S14
FTO/SnO ₂ /CsPbBr ₃ @Cs ₄ PbBr ₆ /carbon	9.02	S15
FTO/c-TiO ₂ /m-TiO ₂ /GOQDs/CsPbBr ₃ /carbon	9.16	This work

S1. Chen S L, Liu X L, Wang Z, Li W H, Gu X Y, Lin J, Yang T Y, Gao X Y, Kyaw A K K. Defect passivation of CsPbBr₃ with AgBr for high-performance all-inorganic

- perovskite solar cells. *Advanced Energy and Sustainability Research*, 2021, 2(6): 2000099
- S2. Liu W W, Liu Y C, Cui C Y, Niu S T, Niu W J, Liu M C, Liu M J, Gu B, Zhang LY, Zhao K. All-inorganic CsPbBr_3 perovskite solar cells with enhanced efficiency by exploiting lone pair electrons via passivation of crystal boundary using carbon nitride ($\text{g-C}_3\text{N}_4$) nanosheets. *Materials Today Energy*, 2021, 21: 100782
- S3. Tak H J, Lee J H, Bae S, J J W. Surface-passivated CsPbBr_3 for developing efficient and stable perovskite photovoltaics. *Crystals*, 2021, 11(12): 1588
- S4. Zuo X X, Chang K, Zhao J, Xie Z Z, Tang H W, Li B, Chang Z R. Bubble-template-assisted synthesis of hollow fullerene-like MoS_2 nanocages as a lithium ion battery anode material. *Journal of Materials Chemistry A*, 2016, 4(1): 51-58
- S5. Duan J L, Dou D W, Zhao Y Y, Wang Y D, Yang X Y, Yuan H W, He B L, Tang Q W. Spray-assisted deposition of CsPbBr_3 films in ambient air for large-area inorganic perovskite solar cells. *Materials today energy*, 2018, 10: 146-152
- S6. Du J, Duan J L, Duan Y Y, Tang Q W. Tailoring organic bulk-heterojunction for charge extraction and spectral absorption in CsPbBr_3 perovskite solar cells. *Science China Materials*, 2021, 64(4): 798-807
- S7. Zhang X S, Jin Z W, Zhang J R, Bai D L, Bian H, Wang K, Sun J, Wang Q, Liu SZ. All-ambient processed binary $\text{CsPbBr}_3-\text{CsPb}_2\text{Br}_5$ perovskites with synergistic enhancement for high-efficiency Cs-Pb-Br-based solar cells. *ACS applied materials & interfaces*, 2018, 10(8): 7145-7154
- S8. Li J, Gao R R, Gao F, Lei J, Wang H X, Wu X, Li J B, Liu H, Hua X D, Liu S Z. Fabrication of efficient CsPbBr_3 perovskite solar cells by single-source thermal evaporation. *Journal of alloys and compounds*, 2020, 818: 152903
- S9. Zhao F, Guo Y X, Wang X, Tao J H, Jiang J C, Hu Z G, Chu J H. Enhanced performance of carbon-based planar CsPbBr_3 perovskite solar cells with room-temperature sputtered Nb_2O_5 electron transport layer. *Solar Energy*, 2019, 191: 263-271
- S10. Liu L L, Yang S E, Liu P, Chen Y S. High-quality and full-coverage CsPbBr_3 thin films via electron beam evaporation with post-annealing treatment for all-inorganic perovskite solar cells. *Solar Energy*, 2022, 232: 320-327
- S11. Zhu J H, Kottokkaran R, Sharikadze S, Gaonkar H, Poly L P, Akopian A, Dalal V L. Inorganic Perovskite Solar Cells with high voltage and excellent thermal and environmental stability. *ACS Applied Energy Materials*, 2022, 5(5): 6265-6273
- S12. Hwang T Y, Choi Y, Song Y S, Emo N S A, Kim S, Cho H B, Myung N V, Choa Y H. A noble gas sensor platform: linear dense assemblies of single-walled carbon nanotubes (LACNTs) in a multi-layered ceramic/metal electrode system (MLES). *Journal of Materials Chemistry C*, 2018, 6(5): 972-979
- S13. Cao X B, Zhang G S, Cai Y F, Jiang L, Chen Y, He X, Zeng Q G, Jia Y, Xing G C, Wei J Q. Enhanced performance of CsPbBr_3 perovskite solar cells by reducing the conduction band offsets via a Sr-modified TiO_2 layer. *Applied Surface Science*, 2020, 529: 147119
- S14. Meng X W, Chi K L, Li Q, Feng B T, Wang H D, Gao T J, Zhou P Y, Yang H B,

Fu W Y. Fabrication of porous lead bromide films by introducing indium tribromide for efficient inorganic CsPbBr_3 perovskite solar cells. *Nanomaterials*, 2021, 11(5): 1253

S15. Liu C B, Zhang T, Li Z, Zhao B H, Ma X T, Chen Y L, Liu Z B, Chen H N, Li X Y. Crystallization kinetics engineering toward high-performance and stable cspbbr_3 -based perovskite solar cells. *ACS Applied Energy Materials*, 2021, 4(10): 10610-10617

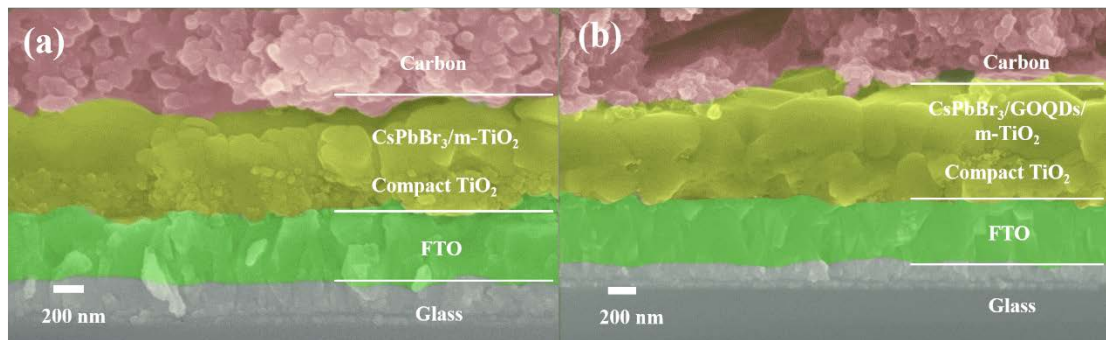


Figure S1. Cross section SEM images of perovskite film (a) without GOQDs and (b) with GOQDs.

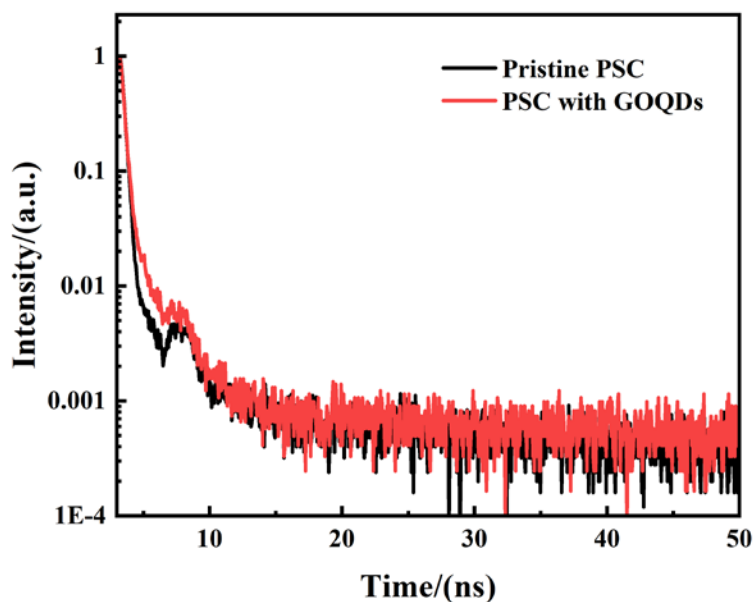


Figure S2. TRPL spectra of the PSCs with and without GOQDs.

Table S2. TRPL key parameters of the PSC with and without GOQDs

PSC devices	τ_1 /(ns)	f1/(\%)	τ_2 /(ns)	f2/(\%)	Tave / (ns)
Pristine	0.27	93.62	4.20	6.38	4.29
PSC with GOQDs	0.29	86.17	2.55	13.83	1.79

Table S3. Hall Effect parameters of the CsPbBr_3 film with and without GOQDs

PSC devices	Resistivity /($\Omega \cdot \text{cm}$)	Bulk concentration /(cm^{-3})	Mobility /($\text{cm}^2 \text{V}^{-1} \text{s}^{-1}$)
Pristine	2.48×10^3	2.45×10^{16}	9.65
PSC with GOQDs	7.13×10^2	5.48×10^{19}	15.97

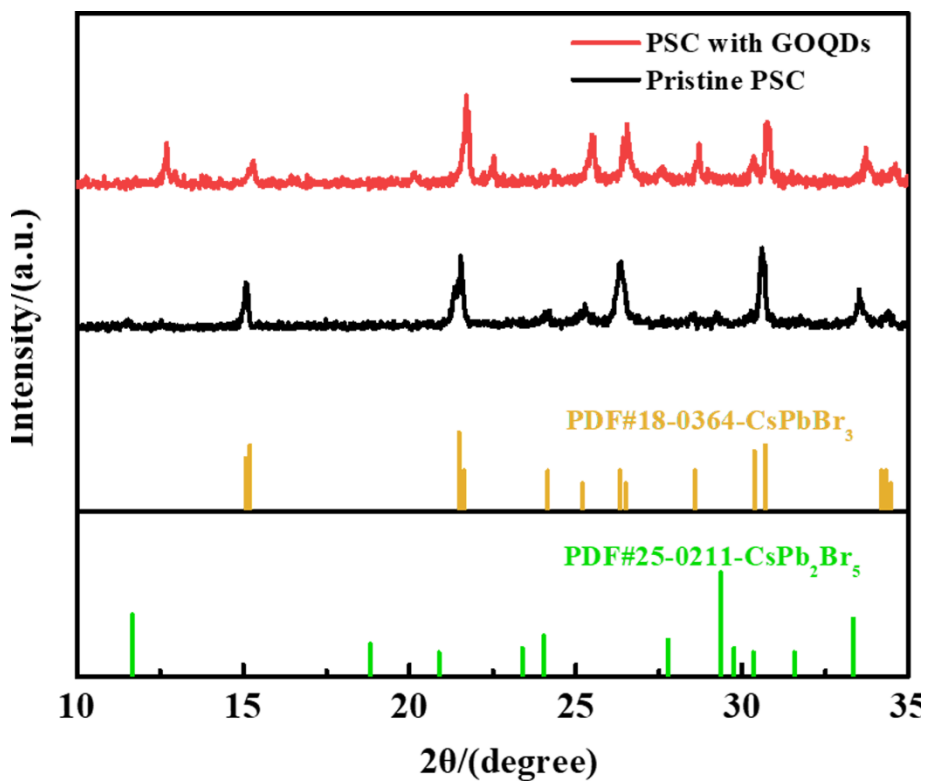


Figure S3. XRD patterns of the PSCs with and without GOQDs.

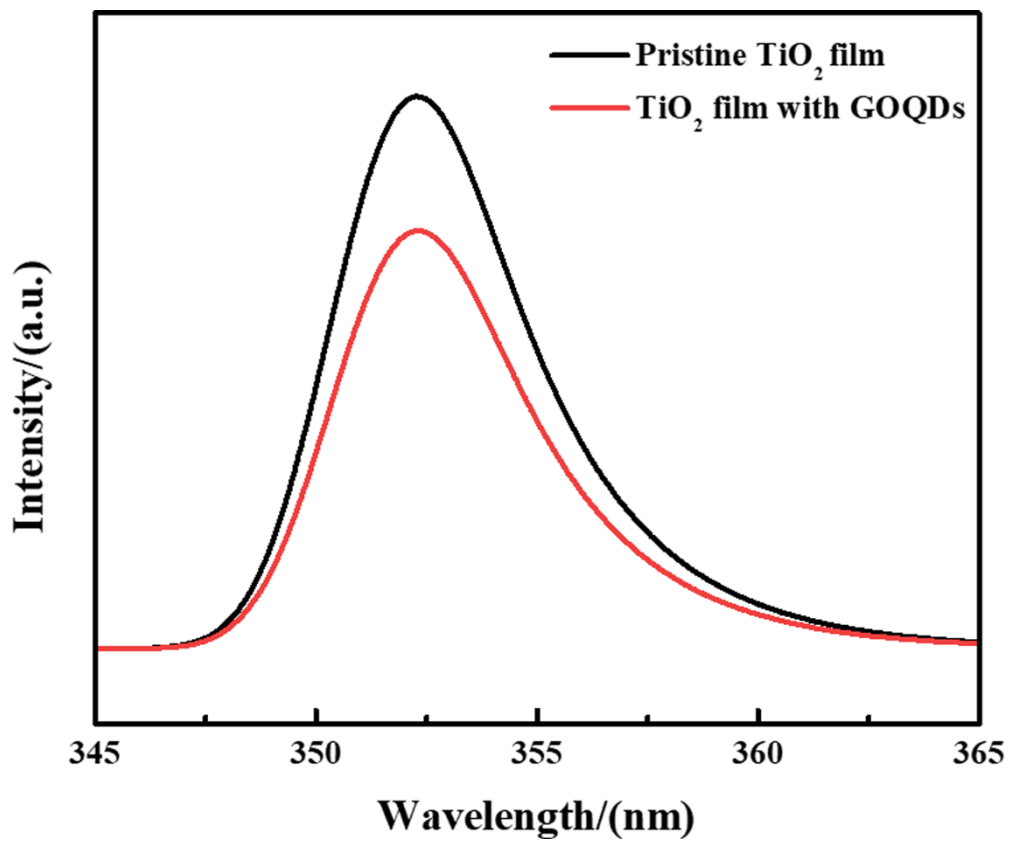


Figure S4. PL spectra of TiO_2 films with and without GOQDs.

Table S4. Hall Effect parameters of the TiO_2 film with and without GOQDs.

TiO_2 film	Resistivity $/(\Omega \cdot \text{cm})$	Bulk concentration $/(\text{cm}^{-3})$	Mobility $/(\text{cm}^2 \text{V}^{-1} \text{s}^{-1})$
Pristine TiO_2 film	4.46×10^3	2.07×10^{12}	66
TiO_2 film with GOQDs	1.04	9.01×10^{16}	67

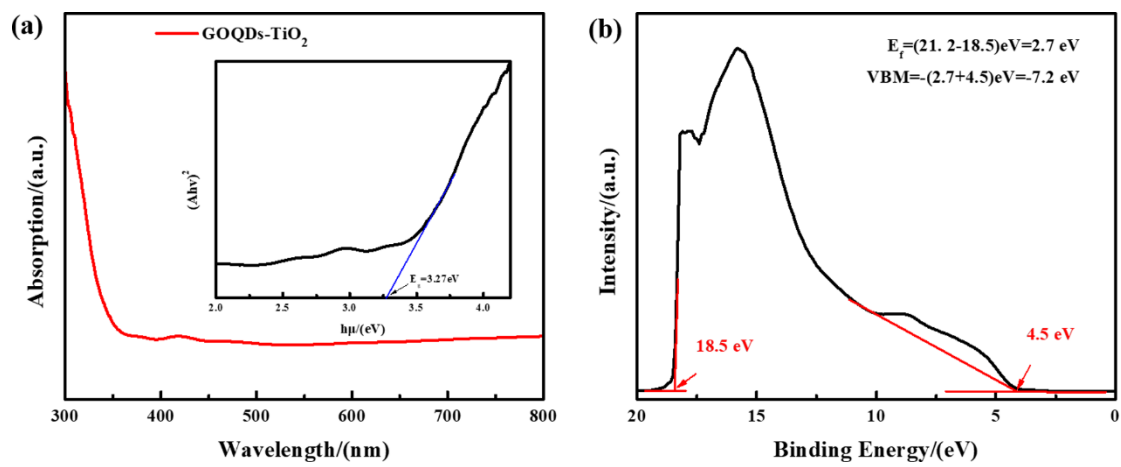


Figure S5 (a) The absorption spectrum of TiO₂ electron transport layer with GOQDs and its corresponding Tauc plot (Inset). (b) The UPS characterization of TiO₂ electron transport layer with GOQDs.

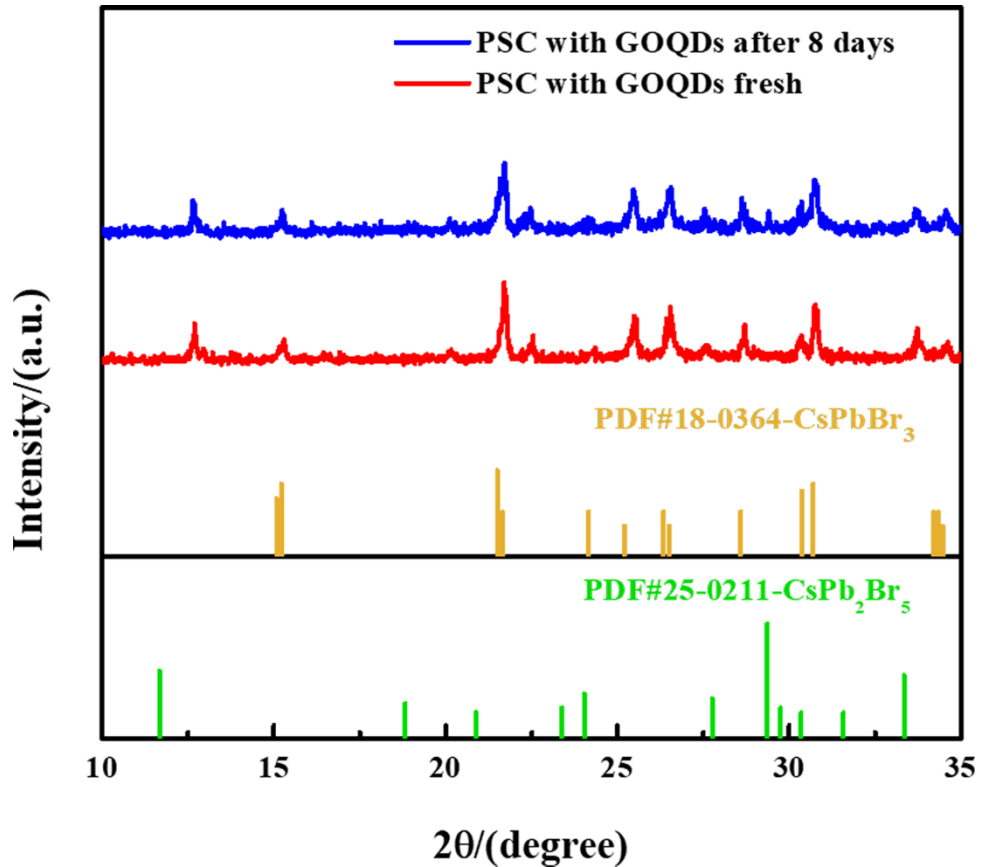


Figure S6. XRD patterns of the PSCs with GOQDs freshly made and after storing in atmosphere for 8 days.